The EMBO Journal vol.10 no.3 pp.521 – 526, 1991

Time-resolved X-ray diffraction study of structural changes associated with the photocycle of bacteriorhodopsin

M.H.J.Koch[1], N.A.Dencher[2,3], D.Oesterhelt[4], H.-J.Plöhn[2], G.Rapp[1] and G.Büldt[2]

[1]European Molecular Biology Laboratory, Hamburg Outstation, EMBL, c/o DESY, Notkestrasse 85, D-2000 Hamburg 52, [2]Department of Physics, Biophysics Group, Freie Universität Berlin, Arnimallee 14, D-1000 Berlin 33, [3]Hahn-Meitner-Institute, Department of Neutron Diffraction I, Glienicker Str. 100, D-1000 Berlin 39 and [4]Max-Planck-Institut für Biochemie, D-8033 Martinsried, FRG

Communicated by D.Oesterhelt

The time course of structural changes accompanying the transition from the M_{412} intermediate to the BR_{568} ground state in the photocycle of bacteriorhodopsin (BR) from *Halobacterium halobium* was studied at room temperature with a time resolution of 15 ms using synchrotron radiation X-ray diffraction. The M_{412} decay rate was slowed down by employing mutated BR Asp96Asn in purple membranes at two different pH-values. The observed light-induced intensity changes of in-plane X-ray reflections were fully reversible. For the mutated BR at neutral pH the kinetics of the structural alterations ($\tau_{1/2}$ = 125 ms) were very similar to those of the optical changes characterizing the M_{412} decay, whereas at pH 9.6 the structural relaxation ($\tau_{1/2}$ = 3 s) slightly lagged behind the absorbance changes at 410 nm. The overall X-ray intensity change between the M_{412} intermediate and the ground state was about 9% for the different samples investigated and is associated with electron density changes close to helix G, B and E. Similar changes ($\tau_{1/2}$ = 1.3–3.6 s), which also confirm earlier neutron scattering results on the BR_{568} and M_{412} intermediates trapped at −180°C, were observed with wild type BR retarded by 2 M guanidine hydrochloride (pH 9.4). The results unequivocally prove that the tertiary structure of BR changes during the photocycle.

Key words: bacteriorhodopsin/conformational change/*Halobacterium halobium*/purple membrane/X-ray synchrotron radiation

Introduction

Recently, neutron diffraction experiments have for the first time established significant reversible structural changes in bacteriorhodopsin (BR), without loss of crystalline order, during the light-induced transition from the BR_{568} ground state to the M_{412} intermediate of the photocycle (Dencher *et al.*, 1989). These changes were observed on native purple membranes (PM), in which the decay of M_{412} to BR_{568}, which under physiological conditions occurs in about 10 ms, was artificially retarded by the presence of 2 M guanidine hydrochloride at alkaline pH. The M_{412} intermediate was then accumulated by illumination at 6°C and stabilized at −180°C. The difference density map ($M_{412}-BR_{568}$) displayed strong peaks at helix G and B and between helix E and F, caused by a shift of the projected density in the neighborhood of both ends of the chromophore retinal during M_{412} formation.

In view of the conflicting evidence regarding the extent of the conformational changes involved in this transition (Ahl and Cone, 1984; Draheim and Cassim, 1985; Frankel and Forsyth, 1985; Glaeser *et al.*, 1986; Dencher *et al.*, 1989) and their importance for the proton pumping mechanism, it would be preferable to observe the changes directly under near physiological conditions and to monitor them kinetically. In order to have a good signal-to-noise ratio in a reasonable data collection time, we have used a mutated BR in purple membrane (Asp96Asn, Soppa and Oesterhelt, 1989). Depending on the pH, the decay of M_{412} in these samples is one to two orders of magnitude slower than in the wild type (Butt *et al.*, 1989), but BR is still fully active as a light-driven proton pump. Taking advantage of the high brilliance of synchrotron radiation sources, the light-induced structural changes in BR could be monitored with a time-resolution of 15 ms under near physiological conditions. This opens a new way to study the structure–function relationship of native and mutated BR at the molecular level.

Results and discussion

The aim of the present investigation was to examine, whether previously described light-induced conformational changes in BR (Dencher *et al.*, 1989) also occur under more physiological conditions and to correlate their kinetics with spectroscopic states of the photocycle. In order to achieve an adequate signal-to-noise ratio within a reasonable measuring time in the time-resolved X-ray experiments, three different BR samples with a retarded M_{412} decay were used: (i) mutated BR Asp96Asn in distilled water (referred to as neutral pH although the actual pH is about 6.0–6.5, due to the negative surface potential of the PM); (ii) mutated BR Asp96Asn at pH 9.6 (100 mM $Na_2CO_3/NaHCO_3$ buffer and 500 mM KCl); and (iii) native BR incubated with 2 M guanidine hydrochloride at pH 9.4 (containing in addition 50 mM $Na_2CO_3/NaHCO_3$ buffer). These samples allow structural comparisons between native and mutated bacteriorhodopsin, as well as the observation of the pH-dependence of the kinetics of conformational alterations.

The diffraction patterns of mutated BR (pH 9.6) in the light-adapted BR_{568} ground state and in the M_{412} intermediate, populated to 100% by continuous illumination, are compared in Figure 1. Data were collected in alternating light and dark intervals of 1 min. The patterns in consecutive 1 min frames either with or without illumination were individually checked for possible sample damage due to light and/or X-rays before averaging. Purple membrane samples are X-ray sensitive as demonstrated by visually observable irreversible bleaching after prolonged exposure. This effect seems even more pronounced upon illumination with visible light. To circumvent this problem the samples were moved

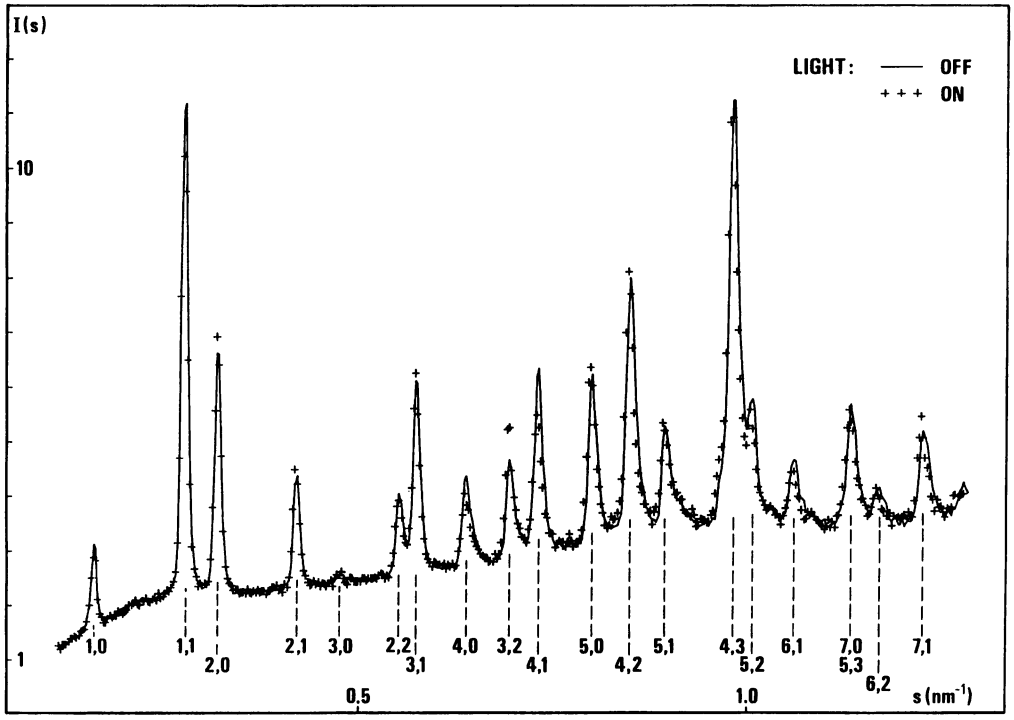

Fig. 1. Diffraction pattern of purple membranes with mutated BR Asp96Asn (pH 9.6, 100 mM carbonate buffer, 0.5 M KCl) in the light-adapted ground state BR_{568} (——) and in the M_{412} intermediate (+++++), obtained in alternating dark and light intervals of 1 min. The total data collection time for each pattern was 20 min. Ordinate: Lorentz corrected intensity I(s); abscissa: scattering vector $s = 2 \cdot \sin\theta/\lambda$. Reflections are indexed on a hexagonal lattice.

several times in the X-ray beam during data collection and only data from intact samples were averaged. Figure 1 exhibits significant intensity variations between the X-ray diffraction pattern of BR in the M_{412} intermediate and in the ground state, with pronounced changes in the (1,1), (3,2) and (4,1) reflections and smaller changes in other reflections (Table I). The overall relative change $\Sigma|\Delta I|/\Sigma I$ in integrated intensity I(s) after Lorentz correction and background subtraction, is about 9%, as also found previously by neutron diffraction (Dencher *et al.*, 1989), corresponding to a value for $\Sigma|\Delta|F||/\Sigma|F|$ of 6%. A 0.4% increase of the hexagonal lattice constant in the M_{412} state was found as in neutron diffraction. The differences in individual reflections and the increase in lattice constant in the M_{412} state were completely reversible and observed in all three types of samples. Model calculations proved that the small difference in the lattice constant of 0.3 Å does not appreciably affect the amplitudes and phases at this resolution and cannot account for the observed intensity changes. No significant changes were found in the lamellar spacing of any of the samples upon exposure to light, indicating that the observed in-plane changes are not due to changes in hydration. The reversibility of the intensity changes during alternating light and dark periods is illustrated in Figure 2 for three reflections. In agreement with Figure 1, the direction of light induced intensity change is opposite for the (3,2) reflection compared to the (1,1) and (4,1) reflections.

As with mutated BR at pH 9.6, similar X-ray intensity changes upon continuous illumination were also observed at room temperature with wild type (ET1001 and GRB) samples treated with 2 M guanidine hydrochloride at pH 9.4 as well as with mutated BR at neutral pH. This confirms the validity of the earlier neutron scattering results (Dencher *et al.*, 1989) and indicates that the observed changes are inherent to the photocycle of BR and are not due to specific features of the mutant, the influence of guanidine hydrochloride, or the high pH.

To ascertain that the observed intensity changes originate from conformational alterations in the protein during the

Table I. Observed powder intensities I_{412} (arbitrary units) and intensity changes between the M-state and the ground state $\Delta I = I_{412} - I_{568}$ together with the errors σ in ΔI

h	k	$h^2 + hk + k^2$	I_{412}	$\Delta I \pm \sigma(\Delta I)$
1	0	1.000	264	− 33 ± 15
1	1	1.732	1723	−164 ± 25
2	0	2.000	997	+ 84 ± 10
2	1	2.646	435	+ 40 ± 10
3	0	3.000	27	+ 5 ± 10
2	2	3.464	352	+ 5 ± 15
3	1	3.606	868	+ 43 ± 15
4	0	4.000	351	− 85 ± 15
3	2	4.359	578	+184 ± 15
4	1	4.583	670	−169 ± 15
5	0	5.000	808	+113 ± 20
3	3	5.196	0	0 ± 20
4	2	5.292	1310	+ 24 ± 20
5	1	5.568	481	+ 34 ± 20
6	0	6.000	56	+ 21 ± 30
4	3	6.083	2475	− 4 ± 30
5	2	6.245	500	− 79 ± 30
6	1	6.557	242	− 70 ± 25
4	4	6.928	0	0 ± 25
7	0	7.000	715	+ 15 ± 25
6	2	7.211	143	− 34 ± 25
7	1	7.550	493	+ 34 ± 25

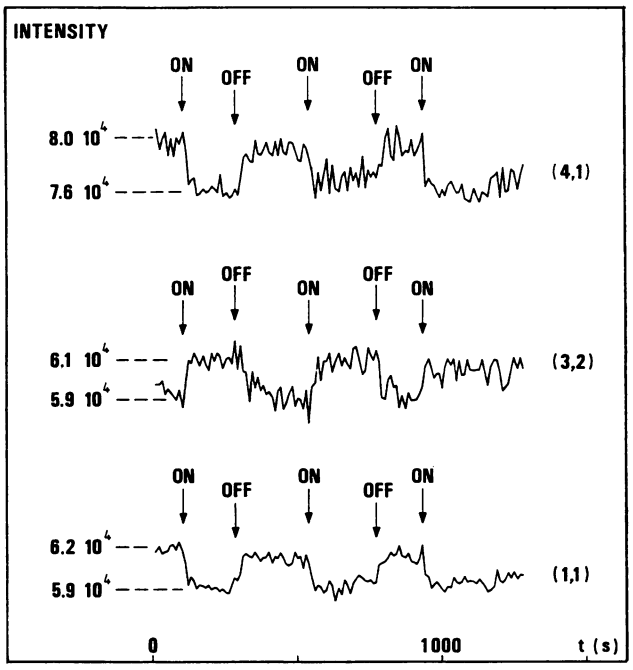

Fig. 2. Reversibility of the changes in the integrated intensity I(s) under the (1,1), (3,2), and (4,1) reflections (i.e. including the background) in the diffraction pattern during dark and light cycles monitored with a 5 s time resolution. The arrows indicate onset and termination of illumination. The curves are displaced for better visualization. Sample: mutated BR Asp96Asn in purple membranes (pH 9.6, 0.1 M carbonate buffer, 0.5 M KCl).

transition from the M_{412} intermediate to the ground state, we have investigated the possible effect of membrane bending on these variations. In suspension, the bending of purple membranes increases during M_{412} formation (Czege, 1988; Drachev *et al.*, 1989). This effect could have caused an increase in the width of the orientational distribution of the PM sheets relative to the mica surface. Such variations could result in changes of integrated intensities since, as a result, the sphere of reflection would intersect different sections along the Bragg rods. This effect was analysed assuming a Gaussian distribution function for the orientation of sheets with FWHM in the range from 0° −20° and using the intensity distribution along Bragg rods determined by electron microscopy (Henderson *et al.*, 1990). Comparison with the observed intensity changes unequivocally excludes this effect as a possible cause for the observed intensity changes.

The intensity increase of some reflections [e.g. (3,2)] proves that one is not dealing with disorder within the unit cell, which would reduce the intensity of the reflections especially at higher resolution and result in a higher Debye−Waller factor. Moreover, as illustrated in Figure 1 and in the bottom curve of Figure 4A, the entire intensity change is due to the ordered part of the structure. The background under the reflections as well as between them remains essentially constant throughout the range of observation.

The diffraction patterns in Figure 1 and the intensity values in Table I can be compared with those obtained using a nanosecond laser plasma source with a wavelength of 0.45 nm (Frankel and Forsyth, 1985). In this case only very poor diffraction patterns were obtained, partly due to the lower resolution of the camera. These patterns display not

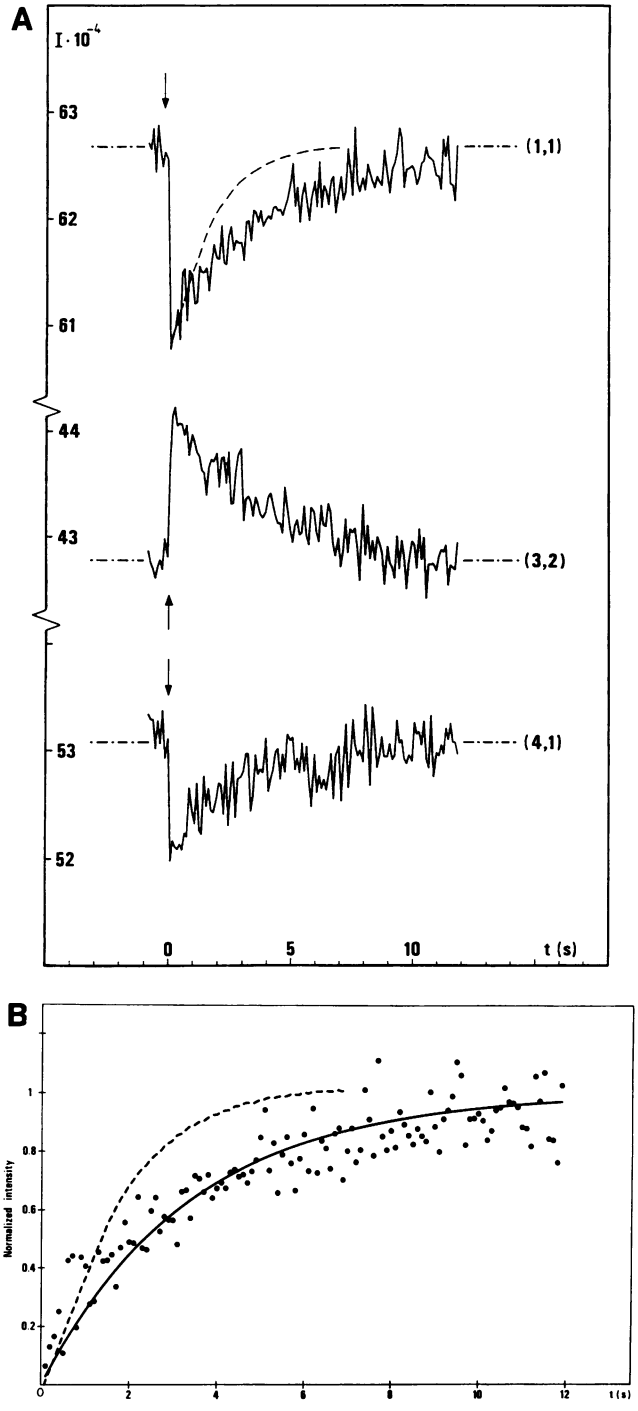

Fig. 3. (**A**) Time course after a short light flash (~0.75 ms FWHM) at t = 0 s of the integrated intensity including background under the (1,1), (3,2), and (4,1) reflections for purple membranes with mutated BR Asp96Asn at pH 9.6 (100 mM carbonate buffer, 500 mM KCl). The data were collected with a time resolution of 100 ms. Absorbance changes at 410 nm (– – – – –) are superimposed on the (1,1) reflection. (**B**) Time course of the X-ray intensity (● ● ● ●) under the (1,1) reflection and of the absorbance at 410 nm (– – – –) together with a single exponential fit with $\tau_{1/2}$ = 3 s through the X-ray data (——). The optical data correspond to $\tau_{1/2}$ = 1 s.

only apparently reversible changes in the (5,0), (4,2), (5,1) and (4,3) reflections but also changes in the (3,2) and (4,1) reflections, not noticed by the authors, that are compatible with our observations. The observed changes and the large increase in background in these experiments were interpreted

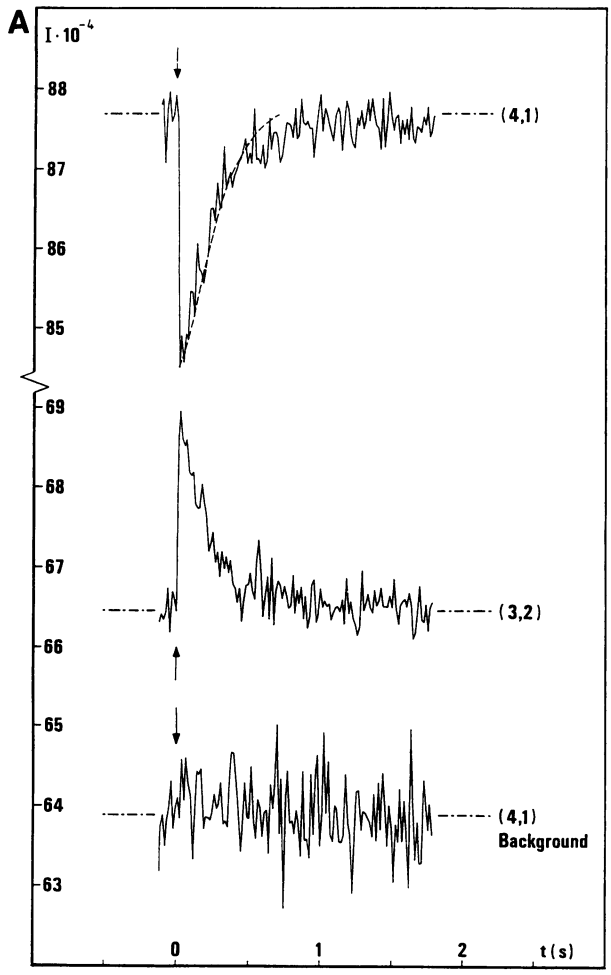

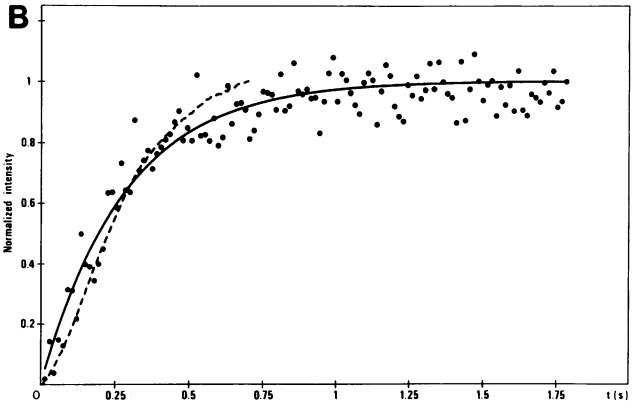

Fig. 4. (**A**) Time course after a short light flash (~0.75 ms FWHM) at t = 0 s of the integrated intensity including background under the (3,2) and (4,1) reflections for mutated BR Asp96Asn at neutral pH in the absence of buffer and KCl. The bottom curve represents the time course of the background under the (4,1) reflection. Data were collected with a time resolution of 15 ms. Absorbance changes at 410 nm (– – – – –) are superimposed on the (4,1) reflection. (**B**) Time course of the X-ray intensity (● ● ● ●) of the (4,1) reflection and of the absorbance at 410 nm (– – – –) together with a single exponential fit with $\tau_{1/2}$ = 125 ms through the X-ray data (——).

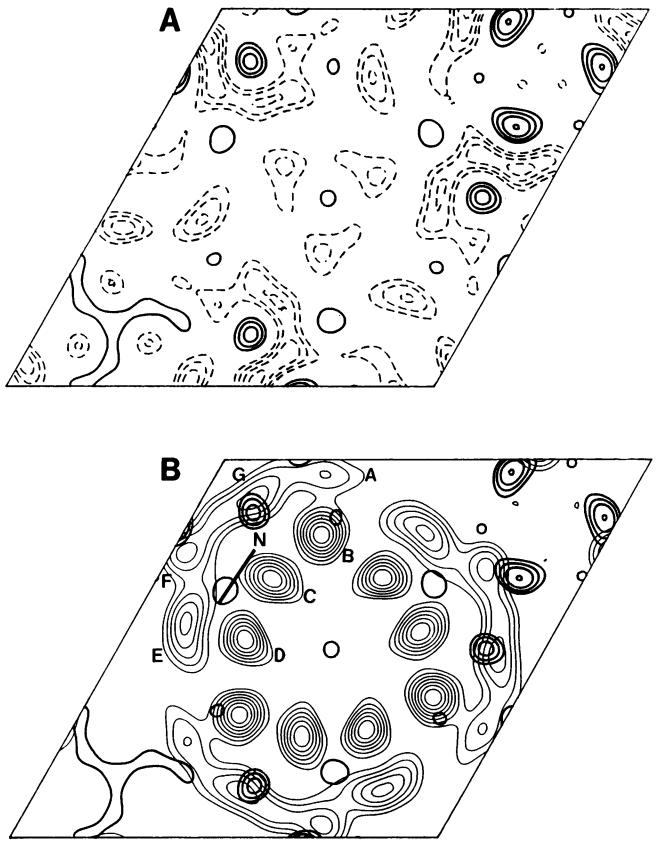

Fig. 5. (**A**) Two-dimensional Fourier map of the difference between the electron density of the M_{412} intermediate and the BR_{568} ground state obtained from the data in Table I. The difference between the maximum and minimum density was set to 100%. The zero difference level corresponds to 43%. The four highest contour lines (——) representing 99, 90, 80 and 70% and the four lowest lines (– – – –) at 30, 20, 10 and 1% are drawn. (**B**) The density levels between 99 and 70% (bold contours) are superimposed on the projected structure of BR in the M_{412} state (thin contour lines). The bold line indicates the in-plane orientation of the chromophore retinal according to Jubb *et al.* (1984), Heyn *et al.* (1988), Büldt *et al.* (1989), and Henderson *et al.* (1990). N marks the position of the Schiff's base nitrogen at the end of the polyene chain of retinal. The helices are assigned according to Dencher *et al.* (1989) and Popot *et al.* (1989).

as resulting from disorder of BR packing in the plane of the purple membrane with little BR structural change.

The time course of flash-induced changes for three reflections in the diffraction pattern of BR Asp96Asn at pH 9.6 is illustrated in Figure 3A. The changes in individual reflections before and immediately after the light flash are consistent with those in Figure 1 and in Table I both in amplitude and in direction. Due to the thickness of some of the samples, only partial conversion to M_{412} was achieved upon flash excitation, resulting in smaller relative intensity changes. The time course of the changes in all reflections can be satisfactorily fitted by a single exponential with the same half-time of about 3 s (Figure 3B). Although some of the X-ray traces seem to deviate from a single exponential, biexponential fits were not applied because of the noise level. The light-induced absorption change at 410 nm, superimposed to that of the (1,1) reflection, however, is faster ($\tau_{1/2}$= 1 s, Figure 3B). Taking into account the initial faster decay time of the X-ray signal (note deviation of the first data points from the fitted 3 s exponential in Figure 3B) and a possible acceleration of the absorbance changes by the strong monitoring light, the temporal difference between both signals might, however, be smaller. [Blue light absorbed by a long living M_{412} intermediate induces a photochemical backreaction to the ground state (Oesterhelt and Hess, 1973; Kalisky *et al.*,

1978)]. This is substantiated by experiments with a less intense 410 nm monitoring beam where the absorbance changes decayed with a predominant (88% amplitude) half-time of 1.4 s (and a second $\tau_{1/2}$ of 4.7 s) as compared to $\tau_{1/2}$ = 2.6 s for the single exponential fit to the corresponding X-ray data.

Comparable data for BR Asp96Asn at neutral pH in the absence of buffer and KCl are presented in Figure 4. Under these conditions, this mutant displays a much faster absorbance decay at 410 nm with a half-time of about 150 ms for the predominant phase (the decay is clearly triphasic, Figure 4B) as compared to 1−1.4 s at pH 9.6. The X-ray intensity decay can be satisfactorily fitted by a single exponential with $\tau_{1/2}$ = 125 ms, i.e. a rate only slightly higher than that of the optical signal (Figure 4B).

The results obtained with two wild type BR samples at pH 9.4 (in the presence of guanidine hydrochloride) also reflect the relaxation of the light-induced structural changes during the M_{412} to BR_{568} transition. In accordance with the data for mutated BR at pH 9.6, the structural relaxation lags behind the first main phase of the absorbance decay at 410 nm (structural changes of the first sample: $\tau_{1/2}$ = 1.3 s, absorbance changes: $\tau_{1/2}$ = 0.65 s, A = 70%, $\tau_{1/2}$ = 3.5 s, A = 24%, $\tau_{1/2}$ = 38.5 s, A = 6%; structural changes of the second sample: $\tau_{1/2}$ = 3.6 s, absorbance changes: $\tau_{1/2}$ = 0.53 s, A = 47%, $\tau_{1/2}$ = 4.3 s, A = 43%, $\tau_{1/2}$ = 57.8 s, A = 10%; weak monitoring light). The first phase of the 410 nm absorbance decay reflects the protonation of the Schiff's base leading to the formation of the N_{550} intermediate. The structural relaxation is slower and therefore occurs after N-formation.

The difference electron density map obtained from the data in Table I is shown in Figure 5. The most pronounced changes occur in the vicinity of helix G and between helices E and F, as also found by neutron diffraction (Dencher *et al.*, 1989). This was observed for all of the samples examined, indicating the importance of structural alterations of the protein in the vicinity of the Schiff's base for the pumping mechanism. It is important to note that the same structural alterations occur in wild type BR and in mutated Asp96Asn BR. At present it cannot be decided, if the additional large density peak emerging predominantly in the lipid area close to helix F, which was not observed by neutron diffraction, reflects true structural changes in BR or is caused by the often found enhancement of noise around the three-fold axis. The difference Fourier map in Figure 5 agrees with respect to the prominent positive density peak at helix G with the one obtained by high-resolution electron diffraction (Glaeser *et al.*, 1986). In electron diffraction significant changes (that were, however, smaller in magnitude) were only found in the resolution range from 5.0−3.3 Å. The present X-ray and recent neutron diffraction results indicate intensity changes in the resolution range 60−7 Å, indicative of alterations in the tertiary structure, such as a small shift or a 1−2° tilt of several helices.

In summary, the X-ray synchrotron data confirm that after the light-induced structural changes generated during the BR_{568} to M_{412} transition (which could not be resolved in time in the present study) BR relaxes to its original conformation during the M_{412} to BR_{568} transition. The fact that the structural relaxation closely corresponds to the absorbance decay at 410 nm, which reflects reprotonation of the Schiff's base, at neutral pH but occurs after the first phase of this decay at alkaline pH (Fig. 3 and 4) suggests that the structure recovers during the N_{550} to BR_{568} transition. This is in agreement with the 'C-T model' (Fodor *et al.*, 1988, Ames and Mathies, 1990). At alkaline pH, the rate of the M_{412} decay in the Asp96Asn mutant decreases strongly, whereas in the wild type the rate of the N_{550} to O_{648} transition is slowed down. This results in changes in the relative concentrations of the M_{412}, N_{550} and O_{648} intermediates (Tittor *et al.*, 1989; Ames and Mathies, 1990, and references cited therein). Consequently, the absorbance changes at 410 nm reflect different events during the M_{412} to BR_{568} transition at neutral (Figure 4) and at alkaline pH (Figure 3, and the data with wild type BR). It can be concluded that during the N_{550} to BR_{568} transition three important molecular events occur: (i) the conformational relaxation of the protein, (ii) reisomerization of the chromophore retinal and (iii) uptake of a cytoplasmic proton by the protein.

Materials and methods

Sample preparation

Purple membranes (PM) were isolated from *Halobacterium halobium* (ET1001) or from wild type *Halobacterium sp. GRB* or its Asp96Asn mutant (strain 326). Mica sheets (15 μm thick) were covered with purple membranes (OD_{568} = 2−4) by slow evaporation of an aqueous suspension at 86% relative humidity and room temperature. To transfer buffer and salt (e.g. guanidine hydrochloride, KCl) into the films, they were soaked for 3−5 h in the corresponding aqueous solutions and thereafter excess solution was removed. The sample cells used for X-ray and absorbance measurements consisted of two mica windows one of which was covered with PM. The small air volume between the windows was kept at about 100% relative humidity. The sample thickness was chosen to allow light excitation of BR and is considerably lower than the optimal thickness, about 1 mm, for 0.15 nm wavelength X-rays.

X-ray diffraction

In-plane, and in some cases, also lamellar diffraction patterns were recorded on the X33 double focusing mirror-monochromator camera of the EMBL in HASYLAB (Koch and Bordas, 1983) on the storage ring DORIS of the Deutsches Elektronen Synchrotron (DESY) at Hamburg. For in-plane diffraction experiments the sample was aligned with the membrane stack perpendicular to the incoming beam. In these conditions, due to the curvature of the Ewald sphere at a wavelength of 0.15 nm, the Bragg rods are intersected at different heights above the h,k-plane at increasing Bragg angles. A sealed linear position sensitive detector with delay line readout, filled with Xe/CO_2 at 2 atm (Gabriel and Dauvergne, 1982), was used with the standard data acquisition system (Boulin *et al.*, 1988). The sample detector distance was 75−100 cm. In order to reduce the background at small angles a sector slit was placed in front of the detector. In this case the signal is proportional to the Lorentz corrected intensity $I(s) = s \cdot i(s)$ with the scattering vector $s = 2 \cdot \sin\theta/\lambda$ and θ the Bragg angle.

For continuous illumination, a halogen lamp (Schott, Mainz, type KL1500, about 20 mW/cm^2) was used. For flash experiments, light from a Xe lamp (Model JML, Rapp and Gueth, 1988) triggered by the data acquisition system was brought onto the sample using a liquid light guide (Oriel, Stratford, CT). Both light sources were equipped with the same filters (Schott GG515 and KG1, about $500 < \lambda < 680$ nm). For each flash of about 0.75 ms duration (FWHM), the system delivered an energy of 10−20 mJ to the sample. The X-ray power absorbed in the sample was estimated to 0.01 mW. The sample was protected from unnecessary X-ray irradiation during the pauses (5 or 10 s), imposed by the repetition rate of the flash, by a fast shutter in front of the specimen triggered by the data acquisition system. During each cycle of a flash experiment, 127 frames of 15 or 100 ms were recorded, the flash being triggered in frame 10. Each frame corresponds to a complete diffraction pattern covering from the (1,0) to the (7,1) reflections. The results of each series of 20 cycles were checked separately. During the course of the experiment the sample was moved to avoid radiation damage. The results of 200−1800 cycles were accumulated depending on signal-to-noise ratio. Static diffraction patterns were recorded in successive 1 min frames except for the data in Figure 2 where 128 time frames of 5 s each were used. The results were analysed using the interactive data evaluation program OTOKO (Boulin *et al.*, 1986). The background was removed by subtracting an eighth degree polynomial fitted through about 50 points between reflections; the peaks and background were integrated in the ranges corresponding to the reflections.

Optical measurements

Before and after the X-ray experiment the flash-induced transmission changes at 410 nm of the various BR samples were measured using the same flash system and filters as for the X-ray experiments. The sample was placed between two interference filters with maximum transmission at 410 nm. One of the filters selected the monitoring light from a 75 W XBO lamp driven by a stabilized power supply (AMCO LTI, Tornesch). The second filter was placed in front of the photodiode (S1337-33BQ, Hamamatsu) monitoring the transmission changes to block off the exciting light. The signal was recorded on a digital oscilloscope (Nicolet 310), stored on disk, and transferred to an IBM PC for further evaluation. As a control, the weaker monitoring light of a Kontron 810 spectrophotometer (2 nm slit) was used to measure the absorbance changes at 410 nm after accumulating the M_{412} intermediate by a short period of continuous illumination with a Schott halogen lamp.

Difference Fourier electron density map

Integrated intensities were obtained from the static X-ray diffraction patterns by fitting single, double, or triple Gaussians with a linear background to the measured reflections. The difference Fourier electron density map was calculated using amplitudes derived from these intensities and phases as well as intensity ratios of overlapping reflections from electron microscopy (Henderson *et al.*, 1986). The greater similarity between the X-ray and electron diffraction patterns should provide a more reliable map than the one obtained with neutrons (Dencher *et al.*, 1989; Plöhn and Büldt, 1986).

Acknowledgements

We thank Dr Klaus Bartels for his help in the initial stage of the experiments and Drs R.Henderson and R.M.Glaeser for helpful discussions, especially their suggestion to investigate the influence of possible mosaic spread changes accompanying M-decay on the integrated intensities. This work has been funded by the German Federal Minister for Research and Technology (BMFT, contract number 03-BU2FUB-3) to G.B. and by the Deutsche Forschungsgemeinschaft (Sfb 312, Projekt B4) to N.A.D.

References

Ahl,P.L. and Cone,R.A. (1984) *Biophys. J.*, **45**, 1039–1049.
Ames,J.B. and Mathies,R.A. (1990) *Biochemistry*, **29**, 7181–7190.
Boulin,C., Kempf,R., Koch,M.H.J. and McLaughlin,S.M. (1986) *Nucl. Instrum. Methods*, **A249**, 399–407.
Boulin,C.J., Kempf,R., Gabriel,A. and Koch,M.H.J. (1988) *Nucl. Instrum. Methods*, **A269**, 312–320.
Büldt,G., Dencher,N.A., Konno,K., Nakanishi,K., Plöhn,H.-J. and Rao,B.N. (1989) *Biophys. J.*, **55**, 225a.
Butt,H.J., Fendler,K., Bamberg,E., Tittor,J. and Oesterhelt,D. (1989) *EMBO J.*, **8**, 1657–1663.
Czege,J. (1988) *FEBS Lett.*, **242**, 89–93.
Dencher,N.A., Dresselhaus,D., Zaccai,G. and Büldt,G. (1989) *Proc. Natl. Acad. Sci. USA*, **86**, 7876–7879.
Drachev,L.A., Kaulen,A.D. and Zorina,V.V. (1989) *FEBS Lett.*, **243**, 5–7.
Draheim,J.E. and Cassim,J.Y. (1985) *Biophys. J.*, **47**, 497–507.
Fodor,S.P.A., Ames,J.B., Gebhard,R., van den Berg,E.M.M., Stoeckenius,W., Lugtenburg,J. and Mathies,R.A. (1988) *Biochemistry*, **27**, 7097–7101.
Frankel,R.D. and Forsyth,J.M. (1985) *Biophys. J.*, **47**, 387–393.
Gabriel,A. and Dauvergne,F. (1982) *Nucl. Instrum. Methods*, **201**, 223–224.
Glaeser,R.M., Baldwin,J., Ceska,T.A. and Henderson,R. (1986) *Biophys. J.*, **50**, 913–920.
Henderson,R., Baldwin,J.M., Downing,K.H., Lepault,J. and Zemlin,F. (1986) *Ultramicroscopy*, **19**, 147–178.
Henderson,R., Baldwin,J.M., Ceska,T.A., Zemlin,F., Beckmann,E. and Downing,K.H. (1990) *J. Mol. Biol.*, **213**, 899–929.
Heyn,M.P., Westerhausen,J., Wallat,I. and Seiff,F. (1988) *Proc. Natl. Acad. Sci. USA*, **85**, 2146–2150.
Jubb,J.S., Worcester,D.L., Crespi,H.L. and Zaccai,G. (1984) *EMBO J.*, **3**, 1455–1461.
Kalisky,O., Lachish,U. and Ottolenghi,M. (1978) *Photochem. Photobiol.*, **28**, 261–263.
Koch,M.H.J. and Bordas,J. (1983) *Nucl. Instrum. Methods*, **A208**, 461–469.
Oesterhelt,D. and Hess,B. (1973) *Eur. J. Biochem.*, **37**, 316–326.
Plöhn,H.-J. and Büldt,G. (1986) *J. Appl. Crystallogr.*, **19**, 255–261.
Popot,J.L., Engelman,D.M., Gurel,O. and Zaccai,G. (1989) *J. Mol. Biol.*, **210**, 829–847.
Rapp,G. and Gueth,K. (1988) *Pfluegers Arch.*, **411**, 200–203.
Soppa,J. and Oesterhelt,D. (1989) *J. Biol. Chem.*, **264**, 13043–13048.
Tittor,J., Soell,C., Oesterhelt,D., Butt,H.J. and Bamberg,E. (1989) *EMBO J.*, **8**, 3477–3482.

Received on October 11, 1990; revised on December 4, 1990